Influence of nanoparticle-ion and nanoparticle-polymer interactions on ion transport and viscoelastic properties of polymer electrolytes

Santosh Mogurampelly, Vaidyanathan Sethuraman, Victor Pryamitsyn, and Venkat Ganesan'

Citation: J. Chem. Phys. **144**, 154905 (2016); doi: 10.1063/1.4946047
View online: http://dx.doi.org/10.1063/1.4946047
View Table of Contents: http://aip.scitation.org/toc/jcp/144/15
Published by the American Institute of Physics

Influence of nanoparticle-ion and nanoparticle-polymer interactions on ion transport and viscoelastic properties of polymer electrolytes

Santosh Mogurampelly,[1] Vaidyanathan Sethuraman,[1] Victor Pryamitsyn,[1] and Venkat Ganesan[2,a)]
[1]*Department of Chemical Engineering, University of Texas at Austin, Austin, Texas 78712, USA*
[2]*Department of Chemical Engineering and Institute for Computational and Engineering Sciences, University of Texas at Austin, Austin, Texas 78712, USA*

(Received 18 February 2016; accepted 1 April 2016; published online 19 April 2016)

We use atomistic simulations to probe the ion conductivities and mechanical properties of polyethylene oxide electrolytes containing Al_2O_3 nanoparticles. We specifically study the influence of repulsive polymer-nanoparticle and ion-nanoparticle interactions and compare the results with those reported for electrolytes containing the polymorph β-Al_2O_3 nanoparticles. We observe that incorporating repulsive nanoparticle interactions generally results in increased ionic mobilities and decreased elastic moduli for the electrolyte. Our results indicate that both ion transport and mechanical properties are influenced by the polymer segmental dynamics in the interfacial zones of the nanoparticle in the ion-doped systems. Such effects were seen to be determined by an interplay between the nanoparticle-polymer, nanoparticle-ion, and ion-polymer interactions. In addition, such interactions were also observed to influence the number of dissociated ions and the resulting conductivities. Within the perspective of the influence of nanoparticles on the polymer relaxation times in ion-doped systems, our results in the context of viscoelastic properties were consistent with the ionic mobilities. Overall, our results serve to highlight some issues that confront the efforts to use nanoparticle dispersions to simultaneously enhance the conductivity and the mechanical strength of polymer electrolyte. *Published by AIP Publishing.* [http://dx.doi.org/10.1063/1.4946047]

I. INTRODUCTION

The design of polymer electrolytes often revolves around the goal of achieving simultaneously enhanced conductivities and mechanical strengths in the same material. Indeed, electrolytes possessing high conductivities but low mechanical strengths exhibit undesirable features such as dendrite formation of the metallic lithium anode which leads to short circuit of the electrodes.[1] Unfortunately, however, factors that enhance the mechanical strength of a material often lead to a deterioration of the conductivity and vice versa.[2–4] Hence, there is an outstanding interest in strategies which can simultaneously enhance both the conductivity and mechanical strength of the electrolyte material.

In the above context, polymer nanocomposites (PNCs), i.e., polymer electrolytes containing nanoscopic ceramic particles, have recently attracted the attention of scientific community.[5–16] Such interest partially stems from reports of enhanced conductivities resulting from the addition of nanoparticles such as TiO_2, SiO_2, Al_2O_3 to polymer electrolytes (SPEs).[9–11,17] Complementing such findings, addition of similar nanofillers to polymer matrices has been shown to lead to significant enhancements in the elastic modulus and mechanical properties of the matrix.[18–20] Together, such observations have piqued an interest in the exploration of the strategy of dispersing nanoparticles as a means to simultaneously achieve the high mechanical strength and conductivity desired in polymer electrolytes.

A number of recent reports have shed light on the different mechanisms underlying ion transport and mechanical properties of PNCs.[5,11,12,16,21–28] Such studies have identified that among the different parameters, nanoparticle surface chemistry serves as a key factor in influencing both of these properties. For instance, Wieczorek *et al.*[29] studied the effect of alumina halides and α-Al_2O_3 nanoparticles on the properties of polymer electrolytes and correlated their conductivity observations to the strength of Lewis acid-base interactions of the nanoparticles with ions. Recently, Maranas and co-workers[30] studied the effect of the surface chemistry of the nanoparticles and found that nanoparticles possessing acidic surface sites result in higher conductivities when compared with nanoparticles containing (roughly) equal numbers of acidic and basic surface sites. Similarly, in the context of mechanical properties, a number of studies have suggested that (for conditions below the percolation threshold of the nanoparticles) the enhancements in elastic moduli arise as a result of polymer-bridged nanoparticle networks formed due to the enthalpic interactions between the polymer and the nanoparticle surfaces.[31–34] Together, such findings have raised the question "can the nanoparticle surface chemistry be tuned to facilitate simultaneous enhancements in the conductivity and mechanical strength of the polymer electrolytes?"

In an effort to clarify the role of nanoparticle surface chemistry upon ionic mobilities, in recent studies we probed the influence of various polymorphs of Al_2O_3 nanoparticles

a)venkat@che.utexas.edu

on the transport properties of ions in polyethylene oxide (PEO) melt solvated with $LiBF_4$ salt.[35,36] While a number of mechanisms were unearthed, the primary mode of influence of the nanoparticles was shown to be through their impact on polymer segmental dynamics. Such effects were in-turn shown to be mediated by an interplay of both the nanoparticle-polymer and nanoparticle-ion interactions. Similar results have also been reported by others for other PNC and nanoparticle-free polymer electrolyte systems.[25,26,37–39]

While the above-discussed studies have contributed fundamental insights, nevertheless, there is still a lack of understanding on general strategies and/or nanoparticle chemistries which lead to an enhancement of the ionic conductivities in PNCs above that of the pristine polymer electrolyte. Motivated by such considerations, the present study seeks to understand the features of nanoparticle surface chemistry which promote an *enhancement* of the ionic mobilities and conductivities of polymer electrolytes. In pursuit of such an objective, we were particularly inspired by a number of other simulation studies which have demonstrated that the presence of repulsive interactions between the polymer and surfaces or nanoparticles can lead to an acceleration of the polymer segmental dynamics.[25,26,40,41] When considered in conjunction with our findings identifying polymer segmental dynamics as a key factor underlying the influence of nanoparticles on ion transport, such results suggest that the nanoparticle chemistries which embody a repulsive component underlying the nanoparticle-polymer and nanoparticle-ion interactions may potentially lead to a robust strategy to achieve conductivity enhancements. Despite the intuitive nature of such a proposal, some unresolved questions confront such an idea:

1. In our earlier studies[35,36] we demonstrated that the polymer segmental dynamics and ion mobilities were influenced by an interplay of *both* the polymer-nanoparticle and ion-nanoparticle interactions. Within this picture, an outstanding question is whether incorporating repulsive polymer-nanoparticle and ion-nanoparticle interactions would necessarily promote acceleration of polymer segmental dynamics and ion mobilities.
2. In an earlier study, we used coarse-grained simulations to probe the transport of penetrants in PNCs.[42] In such a situation, we observed that the diffusion of penetrants was dominated by the so-called "filler" effect, in which the particles act as obstructions for the penetrant diffusion. Interfacial effects, driven by the polymer-nanoparticle interactions, were shown to play only a limited role in modulating the penetrant mobilities even in situations involving repulsive polymer-nanoparticle interactions. Closely related to this is the fact that a number of prior studies have indicated that there exists only a small range of repulsive polymer-nanoparticle interactions wherein a stable dispersion of the nanoparticles can be achieved in the polymer matrix.
3. While the ionic conductivity and diffusion coefficient of the ions are intimately related in the limit of infinitely dilute solution of the ions, at higher salt concentrations, ion correlation effects become important in influencing the conductivities. However, there is little understanding on the influence of nanoparticle-polymer and nanoparticle-ion interactions upon such characteristics and the resulting impact on the conductivity.[27,43–46] These considerations raise the question whether indeed the polymer segmental dynamics can be altered sufficiently within this range of repulsive interactions to enhance the ionic conductivities over and above that of the pristine polymer matrix.
4. Unlike the case of *ion-free* PNCs, which have been extensively studied,[18,31–33,41,47–49] the mechanical properties of *ion-doped* PNCs are expected to reflect the combined influences of polymer-ion, polymer-nanoparticle, and ion-nanoparticle interactions. An outstanding question is the impact of the proposed nanoparticle interactions upon the mechanical properties of the PNCs.

Motivated by the above issues, in the present work, we extend the results of our recent studies[35,36] to probe the influence of *repulsive* polymer-nanoparticle interactions upon both the ionic mobilities and the rheological characteristics. In the present work, we adopt the all atom level parametrized force field used in our earlier work for modeling the polymorph corresponding to β-Al_2O_3 nanoparticles.[35,36] We modify such force-fields to include repulsive interactions representative of the strategy of coating the nanoparticles with neutral ligands or polymer grafts.[27,44–47,49,50] However, instead of modeling such surface functionalization in an atomistically realistic manner, we adopt an *empirical* repulsive potential which can be systematically varied to study the issues discussed above. Within such a framework, we examined a class of interaction potentials with varying strengths of interactions (see Section II B for details) and probed their influence upon the mobilities and mechanical properties. Unfortunately, the time scales underlying atomistic simulations do not allow for an accurate characterization of the thermodynamic stability of the polymer-nanoparticle mixture. However, in our test simulations, when the strength of repulsion was increased beyond a critical value, the simulations, as reflected in the overall system densities, became unstable (see Section IV and Figure S2 of the supplementary material[51] for a discussion of these analyses), and such observations were deemed symptomatic of being thermodynamically immiscible. Using such designed force fields we sought to answer the following questions:

1. Does incorporating additional repulsive interactions between the polymer, ion, and nanoparticles enhance the ionic mobility?
2. Are the ionic mobilities in such designed PNC systems still correlated to polymer segmental dynamics (i.e., what is the importance of the "filler effect")?
3. What is the influence of the repulsive interactions on the correlated ion motion and the conductivity?
4. What is the influence of the polymer-nanoparticle and ion-nanoparticle interactions upon the overall viscoelastic properties of the PNC?

Computer simulations using atomistic force fields enable studies in which the interactions can be varied in a systematic manner to probe the properties of polymer electrolytes.

Unfortunately, however, atomistic simulations are typically expensive for study of mechanical properties and mobilities, thereby rendering it prohibitive to study a wide range of particle volume fractions. To overcome such challenges, we adopt a few methodological innovations arising from our earlier studies.[35,39,48,52–54] For the studies of ion mobilities, we use the methodology of trajectory extending kinetic Monte Carlo (TEKMC)[55] to study the long-time diffusivity of ions in PNC matrices. Such a methodology was adopted in our prior studies and the results were shown to correspond to those arising in long-time atomistic simulations.[35,39,53,54] For studying the viscoelastic properties,[56,57] we draw upon our earlier findings which indicated that at low particle volume fractions, the changes in the viscoelastic properties of PNCs can be obtained by probing the polymer contribution to the rheology arising from relaxation spectra of the normal modes of the polymer chains in the PNC systems.[48,52] To maintain brevity, we present the details of the accompanying methodologies in the supplementary material.[51]

The organization of the rest of the paper is as follows: In Section II, we describe the force field for PEO-$LiBF_4$, interactions of β-Al_2O_3 with PEO-$LiBF_4$, and the modifications we incorporate to accommodate repulsive nanoparticle interactions. This is followed by a description of the test simulations for different force fields and the rationale for the choice of interactions accompanying our studies. In Section III, we present results for the polymer segmental dynamics in *ion-free* systems, the mean squared displacement (MSD) and diffusivity of ionic species in the modified nanoparticle system. This is followed by a discussion of the mechanisms of ion transport in polymer nanocomposites by considering polymer segmental dynamics in *ion-doped* systems and its correlation with ion mobilities. Subsequently, we present the ionic conductivity results and discuss the underlying mechanisms. The viscoelastic properties of the polymer nanocomposites are discussed in Section III E. Finally we present a brief summary in Section IV.

II. COMPUTATIONAL METHODS

A. Interaction potential, system setup, and analysis

Details of the simulation methodology, such as the initial system setup, equilibration, force fields for PEO-$LiBF_4$ electrolyte have been outlined in our previous articles and are adopted for the present study.[35,36] To maintain brevity, here we only briefly summarize the relevant simulation details.

Inspired by the success of the two-body approximation to polarization interactions parameterized by Borodin and Smith,[25,26,58,59] we use the following interaction potential to describe PEO-$LiBF_4$-nanoparticles system:

$$U(\boldsymbol{r}) = U^{\text{bonded}}(\boldsymbol{r}) + A\exp(-Br) - \frac{C}{r^6} + \frac{q_1 q_2}{4\pi\epsilon_0 r} - \frac{D}{r^4}, \qquad (1)$$

where $U^{\text{bonded}}(\boldsymbol{r})$ describes the contribution arising from bonds, angles, and torsions in the PEO. The non-bonded interactions are modeled with second to fifth terms and include the Buckingham potentials (the second and third terms) and the Coulomb potential (4th term). The last term in Eq. (1) represents a two-body, mean-field like dipole polarization interaction. The force field parameters for PEO-$LiBF_4$-nanoparticle electrolyte were borrowed from Refs. 26, 38, and 58 and the static partial atomic charges for atoms in Al_2O_3 nanoparticles were obtained from Ref. 60.

Our simulations considered the PEO matrix containing 40 chains with chemical structure of H-[CH_2-O-CH_2]$_{55}$-H (M_w = 2.425 kg/mol) solvated with 147 Li^+ and BF_4^- ions to obtain a desired salt concentration of EO:Li=15:1. The roughly spherical Al_2O_3 nanoparticles of diameter 14 Å were dispersed in the bulk PEO-$LiBF_4$ melt to generate PNC systems containing 5 and 10 weight percent (wt. %) of the nanoparticles. The PNC systems were simulated at three different temperatures, 500 K, 425 K, and 350 K to understand the thermal effects. All MD simulations were performed using LAMMPS[61] package at constant number of particles, temperature, and pressure (NPT) ensemble to generate a trajectory of 20 ns in each case. The static and dynamic properties (excepting the ion mobilities) were calculated using the last 15 ns of the MD trajectory. For accurate estimation of the diffusivity of ionic species, we extend the MD trajectories to longer time scales using TEKMC simulations[35,36,39,53–55] and the details are given in section V of the supplementary material.[51]

For analyzing the simulation results, we used a variety of static and dynamical measures to understand the mechanisms underlying ion transport in polymer nanocomposites.[35,36] Many of these measures are quite standard in such simulation studies and include characteristics such as the radial distribution functions and mean-squared displacements. To characterize the polymer segmental dynamics, we use the autocorrelation function of dihedral angle involving C–O–C–C atoms, which we denote as $C_{\phi\phi}(t)$.[25,50,51,62,63] We extracted a time scale from the relaxation of $C_{\phi\phi}(t)$ by fitting to a stretched exponential function. In many instances, we also isolate the interfacial effects of the nanoparticles by characterizing the dynamical features in the regions in the proximity to the nanoparticle surface (denoted as "Near" in our results) and in the bulk (denoted as "Far" in our results). For the characterization of viscoelastic properties of the PNC, we rely on the approximation that at low volume fraction of nanoparticles, the viscoelastic response can be obtained as a product of a geometric (hydrodynamic) contribution arising from the particles and a polymer component reflecting the changes in the polymer relaxation.[64,65] To obtain the latter, we effected a normal mode analysis of the trajectories and extract the relaxation spectra of the polymers.[48,52,56,57] To maintain brevity of the text, we relegate the details of the different characterization measures to the supplementary material.[51]

We note that our simulations were performed by keeping the position of the nanoparticles fixed.[35,36] This is expected to be a reasonable approximation since the diffusivities of the nanoparticles are typically much smaller compared to those of polymers and ions in the electrolyte. Nevertheless, to quantify and understand the influence of the dispersion of the nanoparticles, we considered three different distributions of nanoparticle positions for 5 wt. % and 10 wt. % of the loadings. The results of ionic diffusivities and polymer dynamics for different configurations were found to be identical within the error bars (displayed in the results for the temperature of

425 K in Figures 5, 6, 9, and 10). These results confirm that our results are not influenced significantly by the fixing of the locations of the nanoparticles.

B. Modeling of SR-Al_2O_3 nanoparticle interactions

Our objective was to probe the influence of repulsive nanoparticle-polymer interactions upon the conductivities and mechanical properties of the PNCs. Unfortunately, atomistic computer simulations of such characteristics are expensive and preclude a comprehensive study for a wide range of interaction potentials. Instead of pursuing such an effort, we adopted a framework in which we used short time atomistic simulations to investigate the influence of a class of force fields with varying interaction strengths. Among the force fields which resulted in stable configurations (over 10 ns trajectory), for further studies we adopted the specific interactions (which will be denoted henceforth as SR-Al_2O_3) which exhibited the fastest ion dynamics as quantified through their mean-squared displacements. While this protocol may not allow us to address all intricacies arising from the interplay of different interactions, nevertheless, the chosen interactions furnish a satisfactory approach to address majority of the issues raised in the Introduction.

The different test force fields considered in this study are denoted as FF1(SR-Al_2O_3), FF2, FF3, FF4, and FF5 and the interactions corresponding to β-Al_2O_3 are denoted as FF0. Parameters for all of these force fields and partial atomic charges are provided in the supplementary material.[51] The force field for SR-Al_2O_3 nanoparticles is used for all the results presented in Secs. III and IV and is displayed in Figure S1 of the supplementary material for O_{Al} and Al atoms in Al_2O_3 nanoparticles.[51] Briefly, in SR-Al_2O_3, the interactions between the nanoparticles and BF_4^- anions were unchanged from those of β-Al_2O_3 interactions. However, the dispersion interaction parameter C in Eq. (1) for β-Al_2O_3 nanoparticles was set to zero, while the short range repulsive interactions were increased through the parameter B in Eq. (1). We note that similar refinements of the force-field have also been effected in other contexts.[25,26,40,41,66]

Among the other force fields examined, FF2 is closely related to the interactions described by SR-Al_2O_3(FF1) and the remaining set of FFs are closely related to the interactions described by β-Al_2O_3(FF0). Explicitly, FF2 incorporates slightly increased repulsive interactions between the BF_4^- anions and the nanoparticles compared to those of SR-Al_2O_3. FF3 includes increased short-range repulsion between Li^+ ions and O_{Al} atoms of the nanoparticles as well as reduced repulsion of the F atoms of BF_4^- anions with the O_{Al} atoms compared to the corresponding interactions describing β-Al_2O_3 nanoparticles. Similarly, FF4 includes repulsion of EO of the polymer with the nanoparticles in addition to FF3 above. Lastly, FF5 incorporates only the repulsion of Li^+ ions with the nanoparticles compared to that of β-Al_2O_3 nanoparticles. The non-bonded interaction potential that includes short range Buckingham potential as well as the long-range electrostatics for the above described FFs have been shown in Figure 1. In Section IV and Figure S2 of the supplementary material,[51] we present a detailed discussion of the stability issues associated with such interactions and a rationalization for considering the indicated sets of force fields for probing the mobility of the ions.

Test simulations were effected to choose the force field that resulted in the fastest ion mobilities. Such simulations were performed at a nanoparticle loading of 5 wt. % and EO:Li=15:1 at 500 K. Before the production runs with the set of FFs discussed in Section II B, we started with the appropriately equilibrated configuration of the polymer nanocomposite. The interactions of SR-Al_2O_3 and β-Al_2O_3 were then modified to represent the interactions corresponding to FF2, FF3, FF4, and FF5, respectively. Figure 2 displays the MSDs of ions obtained from a 10 ns NPT-MD simulation with the FFx (x = 2, 3, 4, and 5). For comparison, we also display the results obtained in the presence of β-Al_2O_3 and SR-Al_2O_3 nanoparticles. It is seen that the SR-Al_2O_3 nanoparticles result in the most accelerated dynamics of both ions among the force fields considered. However, with FF2, the MSD of Li^+ ions was observed to be close to the case of SR-Al_2O_3 in the subdiffusive regime but lesser at longer time scales. We speculate that for such a case, the BF_4^- ions repelled from the nanoparticles with FF2 tend to form ion-clusters with Li^+ ions. On the other hand, dynamics of ions and polymers with FFx (x = 3, 4, and 5) are close to the case of β-Al_2O_3 nanoparticles. The MSD of Li^+ ions with FF3 seems to be higher than that with FF4 and FF5 in the subdiffusive regime. However, we are unable to generate longer trajectory with FF3 due to large displacement of the BF_4^- ions in a single MD step (caused by large repulsion) even with small time steps. The MSDs in FF4 are higher compared to those seen in FF5, and can be attributed to the stronger repulsive interactions in the FF4 case.

Based on the above results, we adopted the force field corresponding to SR-Al_2O_3 nanoparticles as providing the optimal balance of stability of the system and enhancements in the mobility of the ions. The results presented in Secs. III and IV correspond to such a force field.

III. RESULTS AND DISCUSSION

A. Polymer dynamics in *ion-free* systems

The present work is based on the hypothesis that inclusion of nanoparticles with repulsive interactions within polymer electrolytes will lead to an acceleration of polymer dynamics and a corresponding increase in the mobility of the ions. As a first step towards examining the validity of this proposal, we probed the influence of the nanoparticles on the polymer dynamics in the *ion-free* systems.

In Figure 3, we display the polymer segmental relaxation correlation function $C_{\phi\phi}(t)$ for the *ion-free* PNC system at 425 K and compare it against the corresponding results for the *pure* PEO system. We observe that the polymer segmental relaxations are indeed accelerated in the nanoparticle filled systems when compared to the *pure* PEO system. These effects are directly seen in the monotonic decrease of the average relaxation times with increasing particle loading displayed in the inset of Figure 3. Moreover, the relaxation dynamics of polymer segments in the vicinity of the nanoparticles

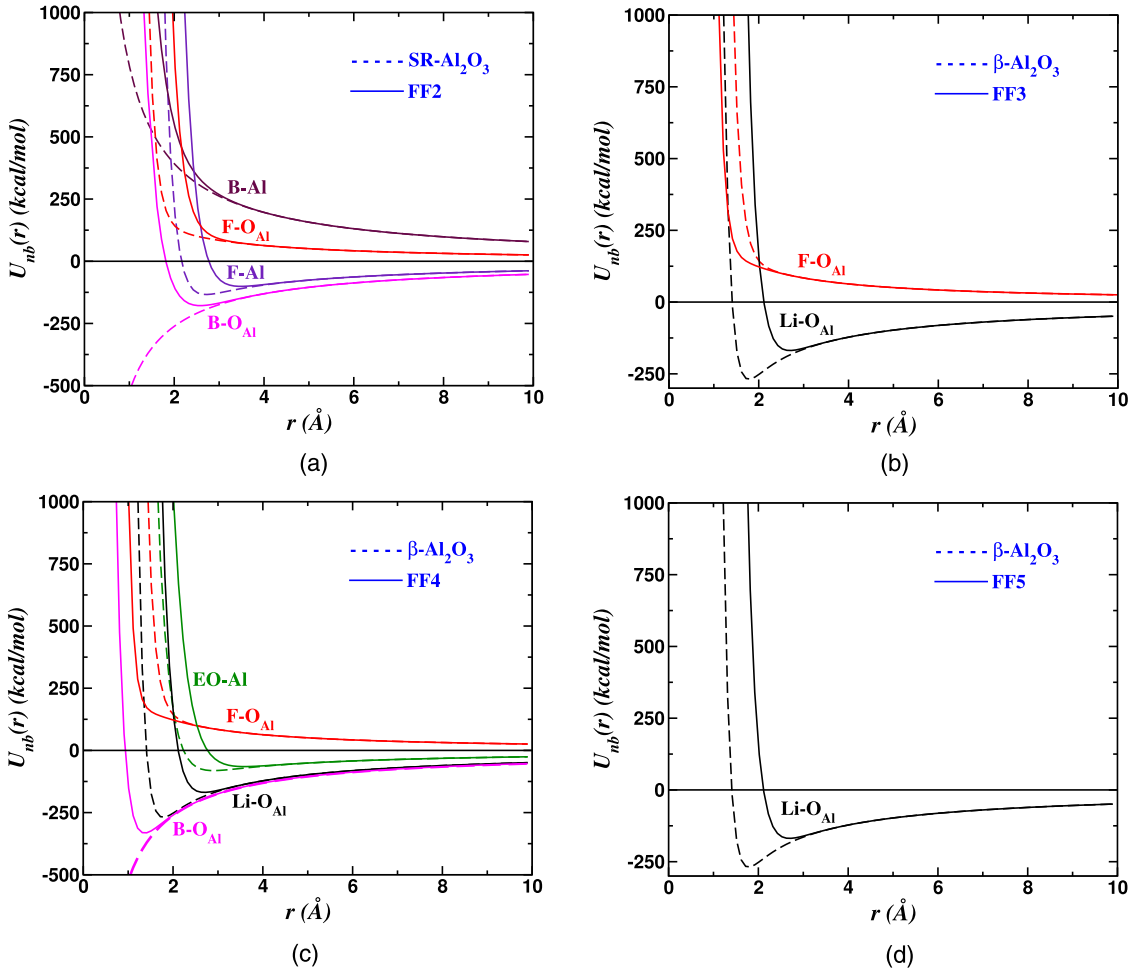

FIG. 1. Approach to the modeling of the non-bonded interactions $U_{nb}(r)$ between Al_2O_3 nanoparticles and PEO-Li^+ melt by SR-Al_2O_3(FF1), FF2, FF3, FF4, and FF5 force fields with respect to β-Al_2O_3. We note that the force fields for β-Al_2O_3 and SR-Al_2O_3 are denoted as FF0 and FF1, respectively, and shown in Figure S1.[51] (a) FF2. (b) FF3. (c) FF4. (d) FF5.

("Near" region in the figure) is seen to be faster than those in the further regions ("Far" in the figure). These results confirm that the acceleration in polymer segmental dynamics arises as a consequence of the interfacial interactions in the polymer-nanoparticle system.

In summary, we observe that the form of the interaction potential we have adopted does lead to an acceleration in the polymer segmental dynamics. This confirms the first hypothesis underlying our work that chemistries embodying repulsive polymer-nanoparticle interactions can

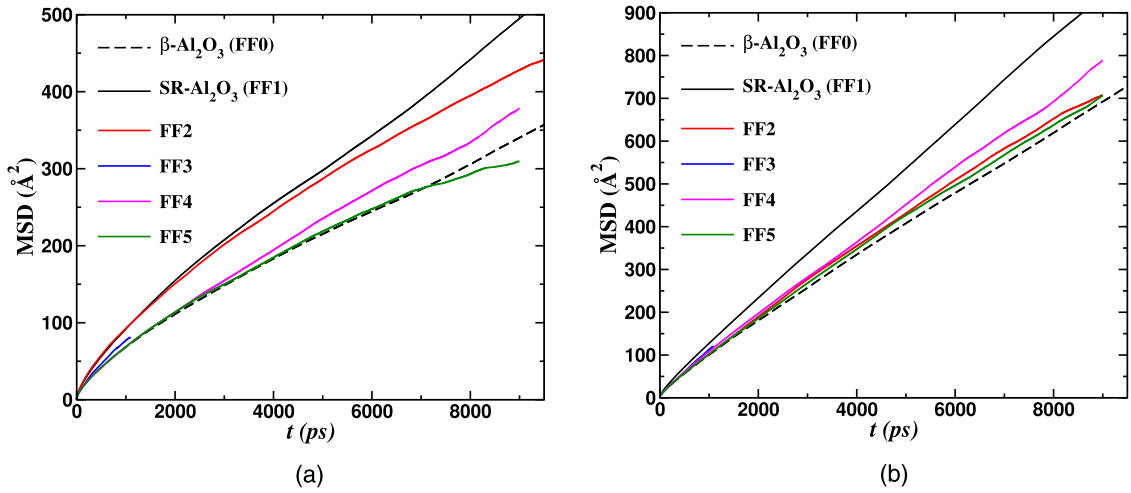

FIG. 2. MSD of ions with various test force fields SR-Al_2O_3(FF1), FF2, FF3, FF4, and FF5 force fields with respect to the original force fields for β-Al_2O_3 nanoparticles. (a) Li^+. (b) BF_4^-.

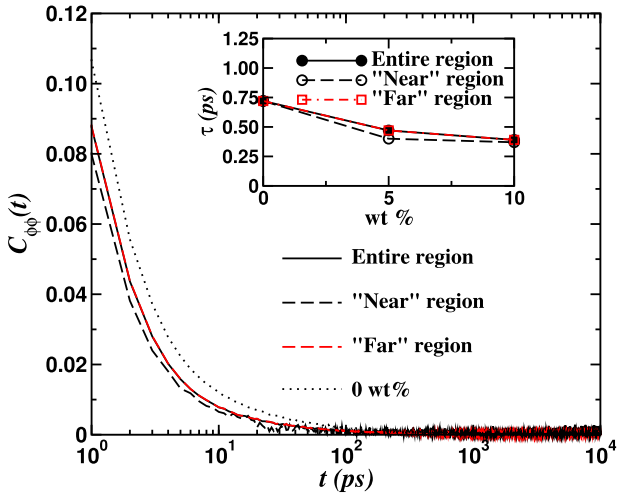

FIG. 3. Dihedral autocorrelation function for PEO chains in the "Near" and "Far" zones at 5 wt. % nanoparticle loading, 425 K for the *ion-free* system. The inset displays the corresponding polymer mean relaxation times.

indeed accelerate the polymer segmental dynamics as compared to the pristine polymer matrix.

B. Ion mobilities

In Figure 4, we present results for the MSD of Li^+ ions in the presence of SR-Al_2O_3 nanoparticles dispersed in PEO-$LiBF_4$ electrolyte at EO:Li=15:1 and 425 K and compare with the corresponding results in nanoparticle-free melt. Also shown for comparison are the MSD results obtained in our previous work[35] for Li^+ ions in the presence of β-Al_2O_3 nanoparticles dispersed in PEO-$LiBF_4$ electrolyte at the same nanoparticle loading. When we compare the results for SR-Al_2O_3 with β-Al_2O_3 nanoparticles, we observe a significant increase in the MSD of Li^+ ions in the former case. Moreover, it is seen that the MSDs in the presence of SR-Al_2O_3 nanoparticles exhibit a monotonic increase with increasing particle loading.

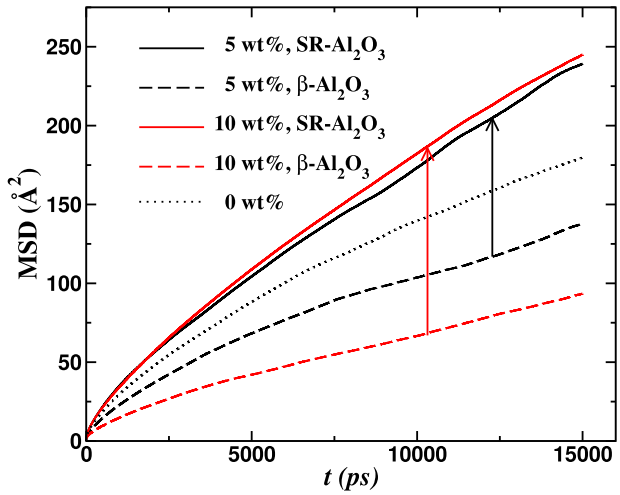

FIG. 4. MSD of Li^+ ions obtained from MD simulations in the presence of SR-Al_2O_3 nanoparticles at a loading of 5 and 10 wt. % at 425 K and EO:Li=15:1 salt concentration. Corresponding data in the presence of β-Al_2O_3 nanoparticles are from our previous work.[35]

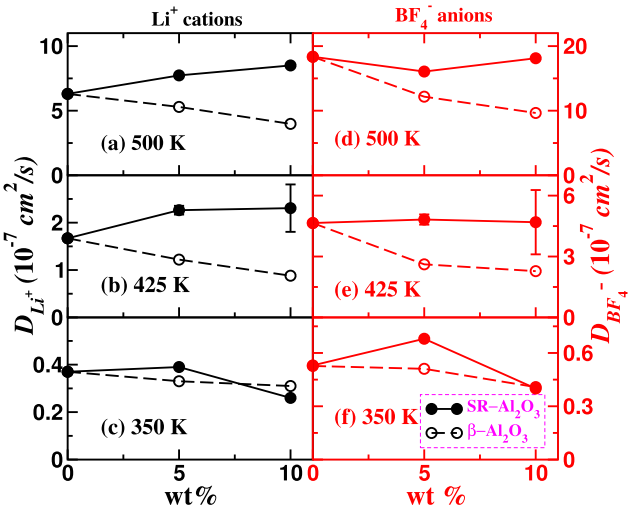

FIG. 5. Diffusion coefficient of Li^+ cations and BF_4^- anions. Data for β-Al_2O_3 are taken from our previous work.[35] Error bars at 425 K and 5 wt. % are comparable to the size of the symbol and lines are guide to the eye.

Figure 5 compares the corresponding diffusivities for cations and anions as a function of the loading of the SR-Al_2O_3 nanoparticles at different temperatures. Results for D_{Li^+} and $D_{BF_4^-}$ in the presence of β-Al_2O_3 nanoparticles (adopted from our previous work[35]) are also shown for comparison. From Figures 5(a)-5(c), we observe that the diffusivity of Li^+ ions increases with increasing temperature, a result broadly consistent with the expectation of increased polymer segmental mobilities at higher temperature. Secondly, we observe that the mobilities of the anions are higher than that of cations, a result also in agreement with our earlier study and other reports.[35,58]

In comparing the ionic diffusivities to nanoparticle-free PEO-$LiBF_4$ melt (0 wt. %) at the temperature of 350 K, we observe that there is a slight enhancement in the mobilities for 5 wt. % loading followed by a slight lowering (relative to the nanoparticle-free melt) at 10 wt. %. In contrast, for temperatures 425 K and 500 K, we observe a monotonic increase in the mobilities with particle loading. However, for all the temperatures, the diffusivities of the cations in SR-Al_2O_3 systems are seen to be higher than the corresponding values in β-Al_2O_3 nanoparticles. The trends for the diffusivity of the anions indicate a more complex behavior, and are nonmonotonic at 350 K and 500 K. However, the diffusivities of the anions in SR-Al_2O_3 systems are still seen to be larger than the corresponding values in β-Al_2O_3 systems.

A number of conclusions and questions can be inferred from the above results. It is evident that the ion diffusivities in SR-Al_2O_3 systems are always higher than those in β-Al_2O_3 polymer electrolytes. This confirms our initial hypothesis that the inclusion of repulsive interactions between the polymer and nanoparticles does indeed enhance the ion mobilities. Moreover, it is clear that the addition of SR-Al_2O_3 nanoparticles can, in some parameter ranges, enhance the ionic mobilities above that of the nanoparticle-free polymer electrolytes. Surprisingly, however, in contrast to the monotonic behavior noted for the polymer segmental dynamics in Section III A, the ion diffusivities are seen

to exhibit nonmonotonic dependence on particle loading at some temperatures. Moreover, for certain parameters, the ion mobilities are lower than the values for nanoparticle-free electrolyte. The mechanisms underlying such behavior will constitute the discussion in Sec. III C.

C. Polymer segmental dynamics in ion-doped systems

In our previous article we demonstrated that as a consequence of the interplay of interactions between polymer, ions, and the nanoparticles, polymer dynamics in *ion-doped* systems can exhibit different characteristics when compared to the behavior in *ion-free* nanoparticle-filled systems. Moreover, ion mobilities in PNC systems were found to correlate more closely to the polymer segmental relaxation times in the *ion-doped* polymer systems rather than the dynamics in *pure* polymer systems. Motivated by such findings, we investigated the polymer dynamics in the *ion-doped* polymer nanocomposites.

In Figure 6, we present results for the polymer segmental relaxation times in *ion-doped* SR-Al_2O_3 nanoparticle systems and compare with the corresponding behaviors in *ion-free* SR-Al_2O_3 systems. Overall, we observe that the segmental relaxations are significantly hindered in the *ion-doped* systems when compared to *ion-free* systems. Such differences in the relaxation times are consistent with the results of other studies,[67–69] and can be understood to be a result of the slowing of the polymer segments induced by coordination with the ionic groups. However, in comparing the particle loading dependencies of polymer dynamics in *ion-doped* and *ion-free* systems, we observe that the mean relaxation time of PEO chains (at 425 K) exhibits a less pronounced dependence on particle loading in the ion-doped systems. To gain further insights into such differences, we probed the spatial dependence of the polymer segmental relaxations, and in Figure 6(b) display the ratio of the segmental relaxations in the "near" and "far" regions. At 5 wt. % loading, we observe that the relative values of the interfacial and bulk dynamics are comparable for ion-doped and ion-free systems. However,

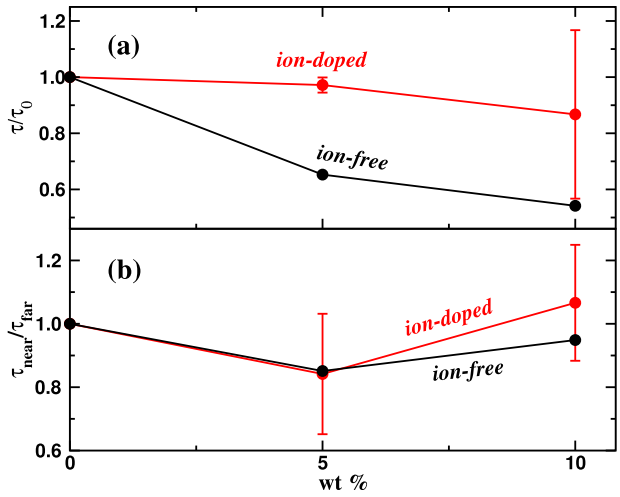

FIG. 6. (a) The mean segmental relaxation time of the *ion-doped* and *ion-free* systems and (b) corresponding behavior in interfacial zone at 425 K.

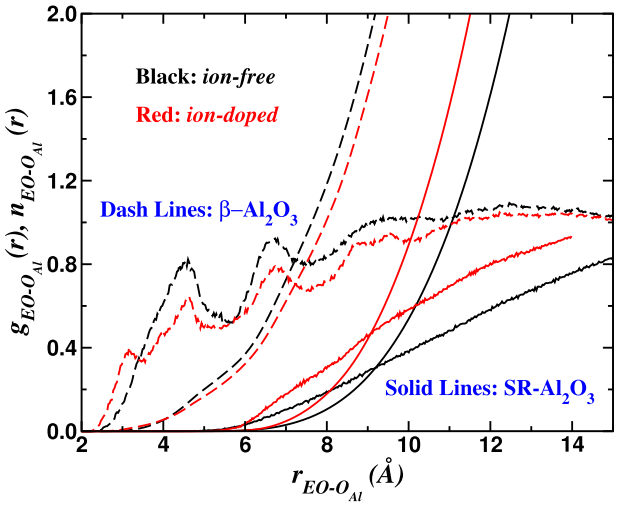

FIG. 7. Partial radial distribution functions for nanoparticle-polymer atomic pairs and the corresponding coordination number for *ion-free* and *ion-doped* systems in the presence of SR-Al_2O_3 and β-Al_2O_3 nanoparticles. The results for the β-Al_2O_3 nanoparticles were adapted from our previous work.[35]

at 10 wt. % loading, we observe that the relative polymer dynamics is slower in the interfacial regions of the ion-doped systems.

The above results broadly point to fundamental differences in the interfacial behavior of the *ion-doped* and *ion-free* PNC systems. To understand the mechanisms underlying such results, we probed the structure of the polymer segments "near" the nanoparticle in both *ion-free* and *ion-doped* systems (shown as $g(r)$ and $n(r)$ in Figure 7). For comparison, we also display the corresponding $g(r)$ and $n(r)$ in the presence of β-Al_2O_3 nanoparticles (adapted from our earlier work, Ref. 35) as dashed lines. In comparing the *ion-free* and *ion-doped* systems in SR-Al_2O_3 systems, we observe that the polymer segments are distributed closer to the nanoparticle surface for the *ion-doped* systems. To rationalize such trends, in Figure 8 we observe that while the Li^+ cations are repelled from the particles (most easily seen by comparing the results for β-Al_2O_3 with SR-Al_2O_3 nanoparticles), the distribution of BF_4^- anions is only slightly influenced by the force field and instead is seen to exhibit a peak near the nanoparticle surface. It now becomes evident that such an anion distribution when coupled with the interactions between the polymer segments and the BF_4^- anions acts as an additional (effective) attraction between the polymer and the nanoparticles in *ion-doped* systems and leads to the differences noted in the polymer segment distributions.

The above structural characteristics also serve to rationalize the differences in the behaviors of interfacial dynamics between the *ion-doped* and *ion-free* systems. Indeed, due to the enhanced density of the polymer segments near the nanoparticles in *ion-doped* systems (relative to *ion-free* systems) the dynamics of polymer segments are expected to be slower near the surfaces. Moreover, we expect the averaged polymer segmental dynamics to reflect a competition between the effects of the repulsive interactions present in SR-Al_2O_3 systems and the anion-induced attractions to the particle surface. At lower temperatures, we expect the latter to dominate and result in slower polymer dynamics

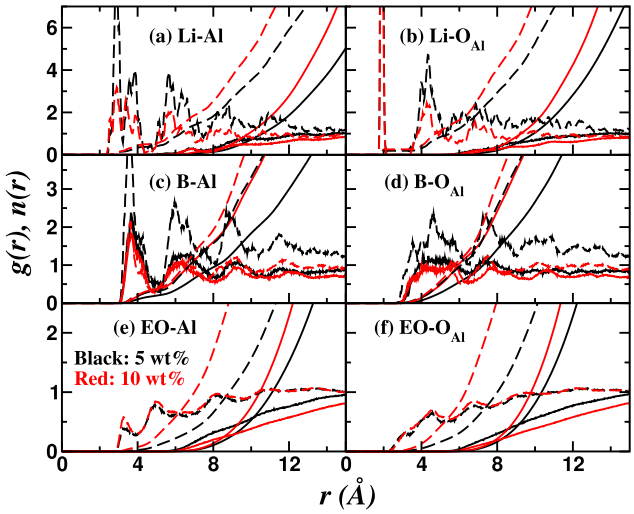

FIG. 8. Radial distribution functions, $g(r)$, and the corresponding coordination numbers, $n(r)$, for various atomic pairs representing partial ((a)-(d)) ion-nanoparticle and ((e)-(f)) polymer-nanoparticle interactions at 500 K. Bold lines indicate PEO-$LiBF_4$ dispersed with SR-Al_2O_3 nanoparticles and dashed lines indicate PEO-$LiBF_4$ dispersed with β-Al_2O_3 nanoparticles. Data for β-Al_2O_3 are adapted from our previous work[35] and shown for comparison.

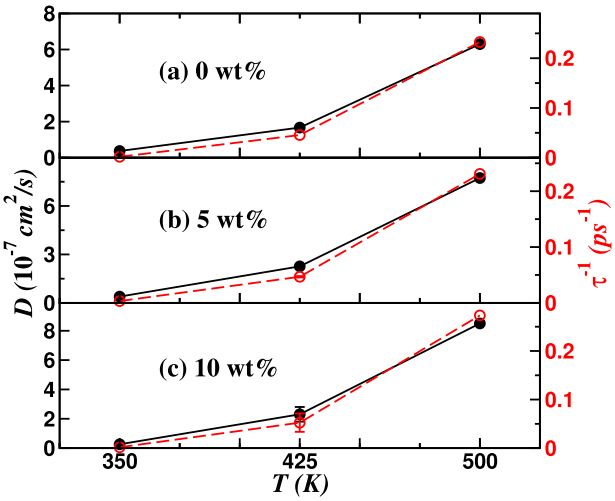

FIG. 9. Correlation between polymer dynamics and diffusion of ions: D of Li^+ ions shown as filled symbols with bold lines and τ^{-1} shown as open symbols with dashed lines as a function of the temperature at various loading of the nanoparticles at EO:Li=15:1. Error bars at 425 K and 5 wt. % are smaller than the size of the symbol.

and cation mobilities. At higher temperatures, we expect the repulsive interactions to dominate and accelerate the overall polymer dynamics (albeit, to a lesser extent relative to *ion-free* systems) and cation mobilities. The anion mobilities are, however, expected to reflect an interplay between the nanoparticle-anion interactions and the polymer segmental dynamics and hence is likely to exhibit a more complex trend for different temperatures and particle loadings. Such considerations rationalize the results presented in Figure 5.

A question that arises from the above results is "what is the origin of the anion distributions around the nanoparticles?" We believe that such effects arise partially due to our adopted force field in which the repulsive component of interactions of the cation and the polymer segments with the nanoparticle were tuned to favor accelerated cation mobilities. However, to maintain stability of the system within such a framework, the nanoparticle-anion interactions had to be correspondingly modulated, which leads to the observed structure for anions. While the results observed are likely specific to our force fields, nevertheless, we do believe that our observations highlight some considerations that transcend the adapted interactions. Indeed, the message that emerges is that while it may be possible to tune the nanoparticle surface chemistry to accelerate the ion and polymer dynamics, there is however a limited range over which such modulations are possible while still maintaining a thermodynamically stable polymer-nanoparticle mixtures. Moreover, while the nanoparticle itself may possess repulsive interactions with the polymer, it is evident that the interplay of nanoparticle-polymer and nanoparticle-ion interactions proves more critical in influencing the structural and dynamical characteristics for the polymer segments in *ion-doped* systems.

Finally, we address the question whether the ionic mobilities in the SR-Al_2O_3 PNC system (Figure 5) are correlated to the polymer segmental dynamics in *ion-doped* systems. In Figure 9, we display the ionic mobilities obtained from our simulations and the (inverse) polymer segmental mobilities as a function of the temperature (the results for other salt concentrations and anions are shown in supplementary material Figure S4[51]). It is observed that there is indeed a very good correlation between the changes in the polymer segmental mobilities in the *ion-doped* systems and the corresponding effects on anionic and cationic mobilities. These results conclusively indicate that the influence of the nanoparticles upon the ionic mobilities can in-turn be attributed to the changes in the polymer segmental dynamics arising from the introduction of nanoparticles in the *ion-doped* systems.[35]

In our previous article, we demonstrated that the above correlation between the polymer segmental dynamics and the ion mobilities was a direct result of the changes in the residence times of the ions in coordination with the polymer segments. To probe if a similar mechanism is operative for the force-fields considered herein, we calculated the residence time autocorrelation function $R(t)$ as a function of the distance from the nanoparticles.[58,70] To maintain brevity, we discuss the results in the supplementary material (Figure S5).[51] Briefly, the results presented therein confirm that the changes in the polymer segmental relaxation times are reflected qualitatively in the residence time correlations of the ions. Explicitly, we show that the residence time correlations in SR-Al_2O_3 nanoparticle systems decay much faster than those in β-Al_2O_3 nanoparticle systems. Moreover, while the residence time correlations near the particles were found to be altered, the results the bulk regions corresponding to the zones away from the particles showed little differences between the particle-free PEO and filled systems.

D. Ionic conductivity of nanocomposites

In this section, we address the influence of the presence of repulsive nanoparticle-polymer interactions upon the ionic conductivities. We recall that ionic conductivity and diffusion

coefficient of the ions are closely related quantities in the situation of infinitely dilute solution of the ions. However, for higher salt concentrations, ion correlation effects such as ion-pairing renders the ionic conductivities to be different from the behaviors exhibited by ionic mobilities. Since ionic conductivity is often the property of interest in polymer electrolytes, it is of relevance to address the influence of the nanoparticle interactions upon such characteristics.

Figures 10(a)-10(c) display ionic conductivities (σ) as a function of the loading of SR-Al_2O_3 nanoparticles at various temperatures. We observe that the conductivity broadly mirrors the qualitative trends observed in the context of ion diffusivities and exhibits enhanced values (relative to particle-free polymer electrolytes) in some regimes of temperature and particle loadings. For all cases, the conductivities in SR-Al_2O_3 systems are seen to be higher than the corresponding values in β-Al_2O_3 systems. However, the enhancements in the conductivity are themselves seen to be more moderate relative to the effects seen in the context of cation diffusivities. In Section III B (Figure 5) we observed that while the cation mobilities exhibited (mostly) monotonic enhancements with particle loadings, the anion mobilities were enhanced in some regimes and lowered in others. Since the conductivity is influenced by the combined values of the cation and anion diffusivities, the magnitudes of change in conductivities can be rationalized to be a consequence of the behaviors exhibited by the individual ion mobilities.

While a major contribution to the changes in the ionic conductivities is expected to arise from the influence of the nanoparticles on the ion mobilities, additional mechanisms may manifest through the changes in the degree of ion "correlations." We explicitly characterize this effect in Figures 10(d)-10(f), through the parameter[71–74] $\bar{\alpha}$ (see the supplementary material[51] Section 1) which embodies the degree of ion correlations. Explicitly, a value of $\bar{\alpha} = 1$ signifies uncorrelated motion of the ions and corresponds to the situation of maximum conductivity, whereas $\bar{\alpha} = 0$ corresponds to the case in which cations and anions move together as ion-pairs giving rise to zero overall conductivity. From the results displayed, we observe that with increased particle loading there is a slight enhancement of $\bar{\alpha}$. These trends can be understood by observing that the radial distribution function plots (Figure 8) displayed differences in the distributions of the anion and cation around the nanoparticle. Explicitly, while cations displayed a depletion around the particles, the anions were not comparably depleted. As a consequence of such differences, there is expected to be an extra dissociation of the salt arising from the presence of nanoparticles and a corresponding increase in the uncorrelated motion of the ions.

The above results suggest that multiple mechanisms underlie the influence of the interactions between nanoparticles and the polymer/ions upon the conductivity of the electrolyte. On the one hand, the nanoparticle-induced modulation of the combined cation *and* anion diffusivities plays an important role. Moreover, the differences in the ion distributions around the nanoparticles influences the degree of dissociation of ions and thereby the degree of correlation in the ion motion.

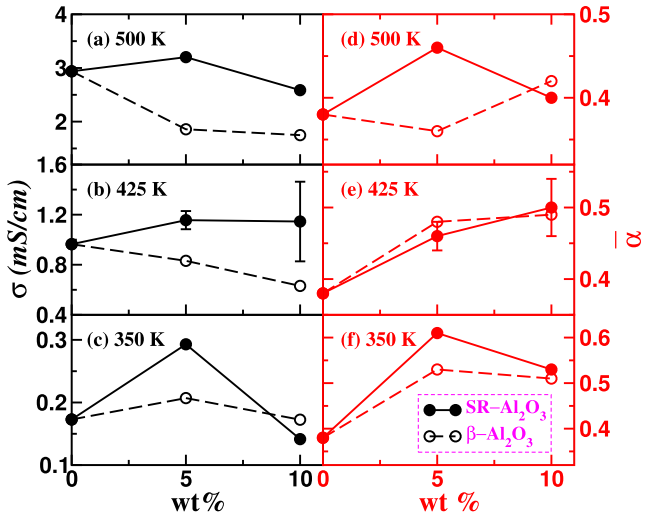

FIG. 10. ((a)-(c)) Ionic conductivity and ((d)-(f)) degree of uncorrelated ion motion for the PEO-$LiBF_4$ electrolyte as a function of the nanoparticles loading at different temperatures. Data for PEO-$LiBF_4$ electrolyte with dispersed β-Al_2O_3 nanoparticles are adapted from our previous work[35] and lines are guide to the eye.

E. Viscoelastic properties

Sections III A–III D demonstrated that the ion mobilities and conductivities of polymer electrolytes can indeed be enhanced by introducing nanoparticle surface chemistries which embody repulsive interactions with the polymer segments and cations. In this final section, we present results for the changes in the viscoelastic properties which result from the introduction of such nanoparticles. In Section I of the supplementary material,[51] we discuss the methodology[48,56,57,75,76] and the approximations[64,65] used to effect the computation of such properties.

The rheological properties $G'(\omega)$ and $G''(\omega)$ for the PNC systems are presented in Figures 11 and 12, respectively. In all cases, we have considered *ion-doped* systems and have compared the nanoparticle-free systems (corresponding to

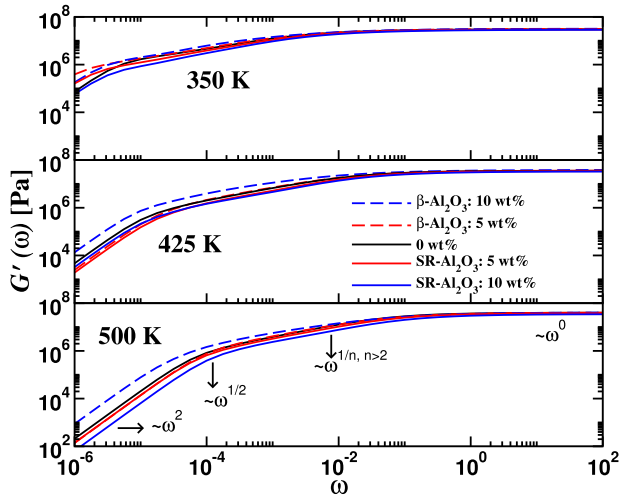

FIG. 11. Storage modulus, G', of the polymer nanocomposite with the loading of SR-Al_2O_3 and β-Al_2O_3 nanoparticles for different temperatures.

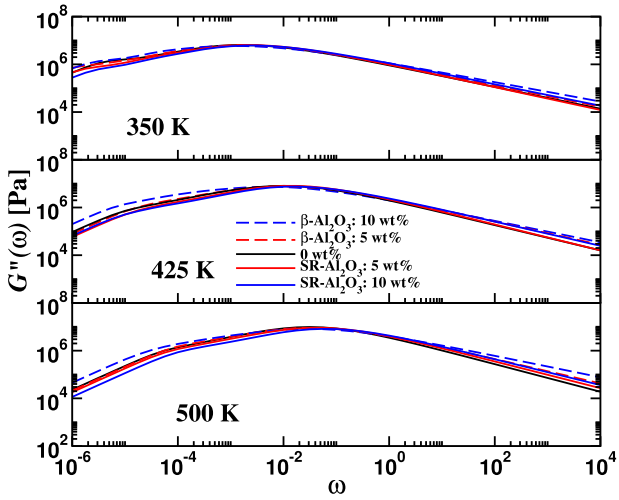

FIG. 12. Loss modulus, G'', of the polymer nanocomposite.

0 wt. %) with the PNC systems containing either SR-Al_2O_3 or β-Al_2O_3 nanoparticles. Broadly, it is observed that the frequency dependent elastic response exhibits characteristics of a Rouse-like polymer melt, with $G'(\omega) \sim \omega^2$ at low frequencies, followed by an intermediate frequency regime with $G'(\omega) \sim \omega^{1/2}$. Such trends are consistent with the short chain lengths considered in our simulations.

To gain further insights into the modulation of rheological properties arising from the introduction of nanoparticles, we employ an idea inspired by the classical time temperature superposition principle. As a first step, we normalize the data for $G'(\omega)$, $G''(\omega)$ to a target reference temperature $T_0 = 350$ K using the time temperature superposition idea. Subsequently, based on the hypothesis that the main influence of nanoparticles on the rheological properties arises through the modulations of polymer dynamics, we employ a "time-particle loading superposition analysis," in which the vertical (moduli) axis is shifted by a factor (denoted as b_W and indicated in Table I) which depends only on the particle loading. Under such shifts (Figures 13 and 14), we observe that $G'(\omega)$ and $G''(\omega)$ for SR-Al_2O_3 and β-Al_2O_3 nanoparticles do individually collapse to a universal function. Except for the small deviations observed at higher frequencies in $G''(\omega)$, which are likely due to the strong interfacial effects arising from the nanoparticle-polymer and nanoparticle-ion interactions, we observe the rheological results obey the superposition hypothesis to a very good approximation. Hence, we use the shift factor b_W as a measure to discuss the influence of the nanoparticles on the mechanical properties.

The inverse of shift factor, b_W, quantifies the magnitude by which the elastic moduli change at a specified loading relative to the particle-free electrolyte. We observe that b_W^{-1} monotonically decreases with particle loading in the case of SR-Al_2O_3 nanoparticles, which indicates a lowering of the mechanical strength relative to the *pure* polymer electrolyte. Moreover, we observe that such reductions become more significant at higher temperatures. In contrast, we observe that b_W^{-1} monotonically increases with particle loading in the case of β-Al_2O_3 nanoparticles, corresponding to an increase in the modulus. The temperature dependence of b_W is seen to be more modest in such cases. The shift factor a_T corresponds to the frequency shifts of the relaxation spectra arising from the introduction of nanoparticles. It is seen that a_T monotonically decreases with particle loading in the case of SR-Al_2O_3 nanoparticles, whereas, in contrast, we observe that a_T increases for β-Al_2O_3 nanoparticles.

The above results are broadly consistent with the trends presented earlier regarding the influence of the respective nanoparticle chemistries upon the polymer segmental relaxation times. Explicitly, in such a context, SR-Al_2O_3 nanoparticles were found to accelerate the polymer dynamics, which reflects in the observed reduction of both a_T and b_W^{-1} with particle loading. However, the surprising aspect in the above results is the more tangible magnitudes and the monotonic nature of the influence of nanoparticles upon the rheological properties which contrasts with the smaller magnitudes and the often nonmonotonic trends observed in the context of ion mobilities. To rationalize such differences, in the supplementary material, we display the spectrum of normal mode relaxations resulting in context of SR-Al_2O_3 nanoparticles (Figure S7).[51] Therein, we observe that with increased particle loading there is a monotonic shift in the time scales of the entire relaxation spectra of the normal modes. Based on such results, we speculate that ion mobilities sample only the short time dynamics of the polymer

TABLE I. Inverse of the vertical shift factors, b_T^{-1} and b_W^{-1}, for the polymer nanocomposite showing the relative decrease/increase of the modulus with the addition of nanoparticles.

		SR-Al_2O_3			β-Al_2O_3		
	T (K)	0	5	10	0	5	10
b_T^{-1}	350	1	1	1	1	1	1
	425	1.164 85	1.154 38	1.146 94	1.164 85	1.158 78	1.200 52
	500	1.312 52	1.280 23	1.199 73	1.312 52	1.292 69	1.283 23
b_W^{-1}	350	1	0.979 27	0.945 67	1	1.026 30	1.053 46
	425	1	0.970 47	0.931 14	1	1.020 95	1.085 72
	500	1	0.955 18	0.864 41	1	1.010 79	1.029 96
a_T	350	1	0.737 40	0.551 43	1	1.085 16	1.000 00
	425	0.174 38	0.106 81	0.098 06	0.162 57	0.138 91	0.247 03
	500	0.041 47	0.038 70	0.023 32	0.051 41	0.045 26	0.071 96

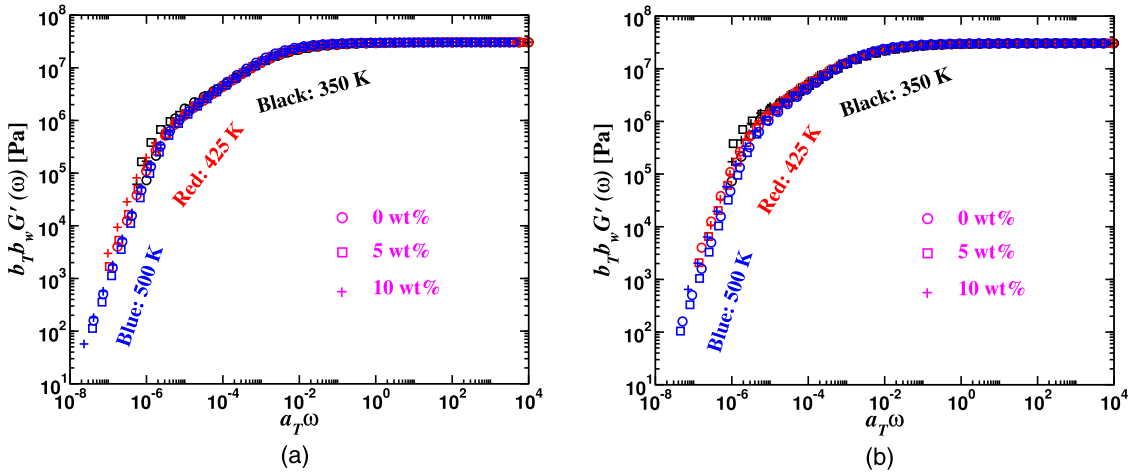

FIG. 13. Master curve for the storage modulus, G', of the polymer matrix to a target temperature 350 K with the loading of (a) SR-Al_2O_3 and (b) β-Al_2O_3 nanoparticles.

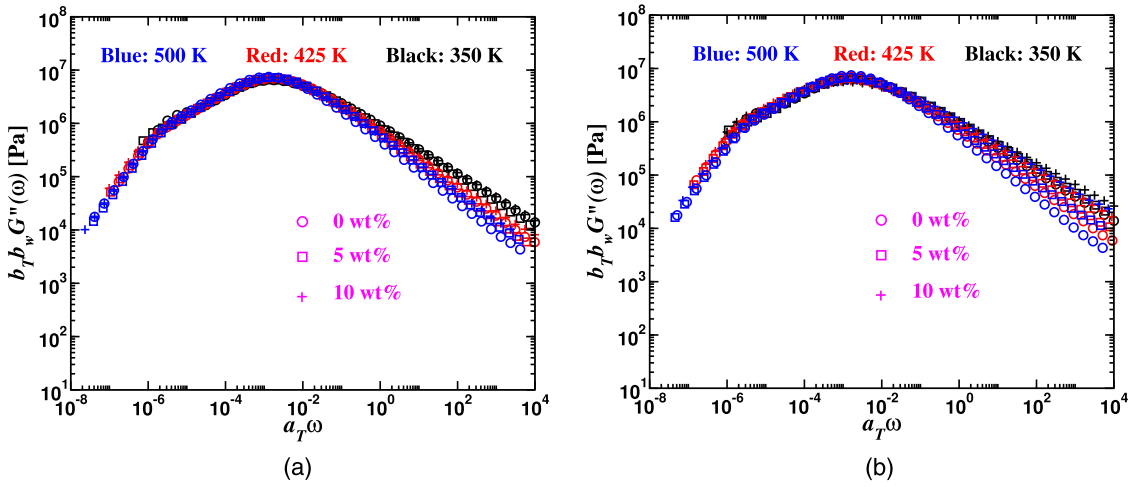

FIG. 14. Master curve for the loss modulus, G'', of the polymer matrix to a target temperature 350 K with the loading of (a) SR-Al_2O_3 and (b) β-Al_2O_3 nanoparticles.

segments, and are hence influenced only to a small extent by the localized changes which occur in the interfacial zone of the nanoparticles. In contrast, the relaxation spectra of the polymer modes average the dynamics of the entire polymer conformations, such that localized disturbances to polymer dynamics can exert a more significant overall influence upon the relaxation times.

IV. CONCLUSIONS

Using all atom molecular dynamics and subsequent trajectory-extending kinetic Monte Carlo simulations, we studied the effect of nanoparticle-polymer/ion interactions upon the conductivity and viscoelastic properties of PEO-$LiBF_4$ electrolyte. The main conclusions which arise from this work are that the inclusion of repulsive nanoparticle/polymer/ion interactions does lead to an increase in the mobilities of the ions and the conductivities relative to the β-Al_2O_3 nanoparticles. However, our results indicate that relative to the particle-free PEO systems the increases in the ion mobilities were more modest and in some cases addition of nanoparticles results in a lowering of such properties. Our results indicate that the mobility of the ions are still correlated to the polymer dynamics in the *ion-doped* PNC systems. More interestingly, our results suggest that the mobility of polymer segments in the *ion-free* systems to be different from those in the *ion-doped* systems and it is the latter which determines the ion mobilities.

Our results in the context of viscoelastic properties were broadly consistent with the ionic mobilities when viewed in the perspective of the influence of nanoparticles on the polymer relaxation times. However, in contrast to the modest influence of the interfacial zones upon the ionic mobilities, the nanoparticles were found to exert a more significant influence on the rheological properties and polymer relaxation spectra.

Overall, our results highlight that similar mechanisms, influenced by nanoparticle-polymer, nanoparticle-ion, and ion-polymer interactions, underlie the changes in the rheological properties and ionic mobilities resulting from the introduction of nanoparticles in polymer matrix. As a consequence, particle chemistries which increase (decrease) the ion mobilities also lower (increase) the mechanical strengths and vice versa. It is to be noted, however, that our results are specific to the system of spherical

or almost spherical nanoparticles dispersed in amorphous polymer melts. In contrast, the properties of PNCs containing anisotropic fillers and/or crystalline polymers are likely to be influenced by other mechanisms, and hence such systems may provide an avenue to simultaneously enhance both the mechanical strengths and the conductivities.

ACKNOWLEDGMENTS

The authors acknowledge the Texas Advanced Computing Center (TACC) at The University of Texas at Austin for providing computing resources that have contributed to the research results reported within this paper. This work was supported in part by grants from Robert A. Welch Foundation (Grant No. F1599) and National Science Foundation (Grant No. DMR-1306844) and the U.S. Army Research Office under Grant No. W911NF-13-1-0396.

[1]K. J. Harry, D. T. Hallinan, D. Y. Parkinson, A. A. MacDowell, and N. P. Balsara, Nat. Mater. **13**, 69 (2014).
[2]P. Bruce and C. Vincent, J. Chem. Soc., Faraday Trans. **89**, 3187 (1993).
[3]J. Song, Y. Wang, and C. Wan, J. Power Sources **77**, 183 (1999).
[4]L. Fan, Z. Dang, C. Nan, and M. Li, Electrochim. Acta **48**, 205 (2002).
[5]M. Armand, Solid State Ionics **9-10**, 745 (1983).
[6]M. B. Armand, Annu. Rev. Mater. Sci. **16**, 245 (1986).
[7]T. E. Springer, T. Zawodzinski, and S. Gottesfeld, J. Electrochem. Soc. **138**, 2334 (1991).
[8]W. H. Meyer, Adv. Mater. **10**, 439 (1998).
[9]F. Croce, G. B. Appetecchi, L. Persi, and B. Scrosati, Nature **394**, 456 (1998).
[10]F. Croce, R. Curini, A. Martinelli, L. Persi, F. Ronci, B. Scrosati, and R. Caminiti, J. Phys. Chem. B **103**, 10632 (1999).
[11]J. M. Tarascon and M. Armand, Nature **414**, 359 (2001).
[12]A. M. Christie, S. J. Lilley, E. Staunton, Y. G. Andreev, and P. G. Bruce, Nature **433**, 50 (2005).
[13]A. S. Arico, P. G. Bruce, B. Scrosati, J. M. Tarascon, and W. Van Schalkwijk, Nat. Mater. **4**, 366 (2005).
[14]P. G. Bruce, B. Scrosati, and J.-M. Tarascon, Angew. Chem., Int. Ed. **47**, 2930 (2008).
[15]B. Smitha, S. Sridhar, and A. A. Khan, J. Membr. Sci. **259**, 10 (2005).
[16]D. T. Hallinan, Jr. and N. P. Balsara, Annu. Rev. Mater. Res. **43**, 503 (2013).
[17]S. K. Fullerton-Shirey and J. K. Maranas, J. Phys. Chem. C **114**, 9196 (2010).
[18]R. Krishnamoorti and E. Giannelis, Macromolecules **30**, 4097 (1997).
[19]M. A. Rafiee, J. Rafiee, Z. Wang, H. Song, Z.-Z. Yu, and N. Koratkar, ACS Nano **3**, 3884 (2009).
[20]C. Tang, K. Hackenberg, Q. Fu, P. M. Ajayan, and H. Ardebili, Nano Lett. **12**, 1152 (2012).
[21]C. Berthier, W. Gorecki, M. Minier, M. B. Armand, J. M. Chabagno, and P. Rigaud, Solid State Ionics **11**, 91 (1983).
[22]C. Angell, Solid State Ionics **18-9**, 72 (1986).
[23]M. A. Ratner and D. F. Shriver, Chem. Rev. **88**, 109 (1988).
[24]F. Müller-Plathe, Acta Polym. **45**, 259 (1994).
[25]O. Borodin, G. D. Smith, R. Bandyopadhyaya, and E. Byutner, Macromolecules **36**, 7873 (2003).
[26]O. Borodin, G. D. Smith, R. Bandyopadhyaya, P. Redfern, and L. A. Curtiss, Modell. Simul. Mater. Sci. Eng. **12**, S73 (2004).
[27]V. Ganesan and A. Jayaraman, Soft Matter **10**, 13 (2014).
[28]S. Mogurampelly, O. Borodin, and V. Ganesan, Annu. Rev. Chem. Biomol. Eng. **7**, 15.1 (2016).
[29]W. Wieczorek, A. Zalewska, D. Raducha, Z. Florjanczyk, and J. R. Stevens, J. Phys. Chem. B **102**, 352 (1998).
[30]L. V. N. R. Ganapatibhotla and J. K. Maranas, Macromolecules **47**, 3625 (2014).
[31]Q. Zhang and L. Archer, Langmuir **18**, 10435 (2002).
[32]Q. Zhang and L. Archer, Macromolecules **37**, 1928 (2004).
[33]M. Surve, V. Pryamitsyn, and V. Ganesan, Phys. Rev. Lett. **96**, 177805 (2006).
[34]Q. Chen, S. Gong, J. Moll, D. Zhao, S. K. Kumar, and R. H. Colby, ACS Macro Lett. **4**, 398 (2015).
[35]S. Mogurampelly and V. Ganesan, Macromolecules **48**, 2773 (2015).
[36]S. Mogurampelly and V. Ganesan, Solid State Ionics **286**, 57 (2016).
[37]H. Kasemägi, M. Klintenberg, A. Aabloo, and J. O. Thomas, J. Mater. Chem. **11**, 3191 (2001).
[38]H. Kasemägi, M. Klintenberg, A. Aabloo, and J. O. Thomas, Solid State Ionics **147**, 367 (2002).
[39]B. Hanson, V. Pryamitsyn, and V. Ganesan, ACS Macro Lett. **2**, 1001 (2013).
[40]F. W. Starr, T. B. Schroder, and S. C. Glotzer, Macromolecules **35**, 4481 (2002).
[41]G. Smith, D. Bedrov, L. Li, and O. Byutner, J. Chem. Phys. **117**, 9478 (2002).
[42]V. Pryamitsyn, B. Hanson, and V. Ganesan, Macromolecules **44**, 9839 (2011).
[43]J. Smith, D. Bedrov, and G. Smith, Compos. Sci. Technol. **63**, 1599 (2003).
[44]S. E. Harton and S. K. Kumar, J. Polym. Sci., Part B: Polym. Phys. **46**, 351 (2008).
[45]P. Akcora, H. Liu, S. K. Kumar, J. Moll, Y. Li, B. C. Benicewicz, L. S. Schadler, D. Acehan, A. Z. Panagiotopoulos, V. Pryamitsyn, V. Ganesan, J. Ilavsky, P. Thiyagarajan, R. H. Colby, and J. F. Douglas, Nat. Mater. **8**, 354 (2009).
[46]V. Pryamtisyn, V. Ganesan, A. Z. Panagiotopoulos, H. Liu, and S. K. Kumar, J. Chem. Phys. **131**, 221102 (2009).
[47]G. D. Hattemer and G. Arya, Macromolecules **48**, 1240 (2015).
[48]V. Pryamitsyn and V. Ganesan, Macromolecules **39**, 844 (2006).
[49]S. A. Kim, R. Mangal, and L. A. Archer, Macromolecules **48**, 6280 (2015).
[50]T. V. M. Ndoro, M. C. Boehm, and F. Müller-Plathe, Macromolecules **45**, 171 (2012).
[51]See supplementary material at http://dx.doi.org/10.1063/1.4946047 for details regarding (i) the characterization measures used in simulations, (ii) repulsive interaction potentials describing SR-Al_2O_3 nanoparticle force fields, (iii) protocol used in equilibration of the simulations, (iv) demonstration of instability of PEO-$LiBF_4$ electrolyte with large repulsive interactions, (v) TEKMC method, (vi) correlation between polymer dynamics and ion mobilities, (vii) residence time autocorrelation functions in different interfacial zones, (viii) radial distribution functions between various components of polymer-salt, (ix) relaxation spectrum of the normal modes, and (x) parameters for all the force fields considered.
[52]J. M. Kropka, K. W. Putz, V. Pryamitsyn, V. Ganesan, and P. F. Green, Macromolecules **40**, 5424 (2007).
[53]B. Hanson, V. Pryamitsyn, and V. Ganesan, J. Phys. Chem. B **116**, 95 (2012).
[54]D. Kipp and V. Ganesan, J. Appl. Phys. **113**, 234502 (2013).
[55]S. Neyertz and D. Brown, Macromolecules **43**, 9210 (2010).
[56]P. E. Rouse, J. Chem. Phys. **21**, 1272 (1953).
[57]M. Doi and S. F. Edwards, *The Theory of Polymer Dynamics*, International Series of Monographs on Physics (Oxford University Press, New York, 1988).
[58]O. Borodin, G. D. Smith, and R. Douglas, J. Phys. Chem. B **107**, 6824 (2003).
[59]O. Borodin and G. D. Smith, J. Phys. Chem. B **107**, 6801 (2003).
[60]J. Sarsam, M. W. Finnis, and P. Tangney, J. Chem. Phys. **139**, 204704 (2013).
[61]S. Plimpton, J. Comput. Phys. **117**, 1 (1995).
[62]G. D. Smith, O. Borodin, D. Bedrov, W. Paul, X. H. Qiu, and M. D. Ediger, Macromolecules **34**, 5192 (2001).
[63]G. D. Smith, O. Borodin, and W. Paul, J. Chem. Phys. **117**, 10350 (2002).
[64]H. Smallwood, J. Appl. Phys. **15**, 758 (1944).
[65]E. Guth, J. Appl. Phys. **16**, 20 (1945).
[66]F. W. Starr, T. B. Schroder, and S. C. Glotzer, Phys. Rev. E **64**, 021802 (2001).
[67]M. Vogel and T. Torbruegge, J. Chem. Phys. **125**, 054905 (2006).
[68]M. Vogel and T. Torbruegge, J. Chem. Phys. **125**, 164910 (2006).
[69]S. K. Fullerton-Shirey and J. K. Maranas, Macromolecules **42**, 2142 (2009).
[70]H. Wu, O. T. Cummings, and C. D. Wick, J. Phys. Chem. B **116**, 14922 (2012).
[71]O. Borodin, W. Gorecki, G. D. Smith, and M. Armand, J. Phys. Chem. B **114**, 6786 (2010).
[72]Z. Li, G. D. Smith, and D. Bedrov, J. Phys. Chem. B **116**, 12801 (2012).
[73]V. Lesch, S. Jeremias, A. Moretti, S. Passerini, A. Heuer, and O. Borodin, J. Phys. Chem. B **118**, 7367 (2014).
[74]J. Picalek and J. Kolafa, J. Mol. Liq. **134**, 29 (2007).
[75]K. Kremer and G. Grest, J. Chem. Phys. **92**, 5057 (1990).
[76]V. Pryamitsyn and V. Ganesan, J. Rheol. **50**, 655 (2006).